

One Point is All You Need: Directional Attention Point for Feature Learning

Liqiang Lin¹ Pengdi Huang¹ Chi-Wing Fu² Kai Xu³ Hao Zhang⁴ Hui Huang¹

¹Shenzhen University

²The Chinese University of Hong Kong

³National University of Defense Technology

⁴Simon Fraser University

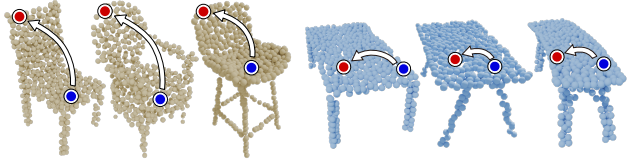
Abstract

We present a novel attention-based mechanism for learning enhanced point features for tasks such as point cloud classification and segmentation. Our key message is that if the right attention point is selected, then “one point is all you need”—not a sequence as in a recurrent model and not a pre-selected set as in all prior works. Also, where the attention point is should be learned, from data and specific to the task at hand. Our mechanism is characterized by a new and simple convolution, which combines the feature at an input point with the feature at its associated attention point. We call such a point a directional attention point (DAP), since it is found by adding to the original point an offset vector that is learned by maximizing the task performance in training. We show that our attention mechanism can be easily incorporated into state-of-the-art point cloud classification and segmentation networks. Extensive experiments on common benchmarks such as Model-Net40, ShapeNet-Part, and S3DIS demonstrate that our DAP-enabled networks consistently outperform the respective original networks, as well as all other competitive alternatives, including those employing pre-selected sets of attention points.

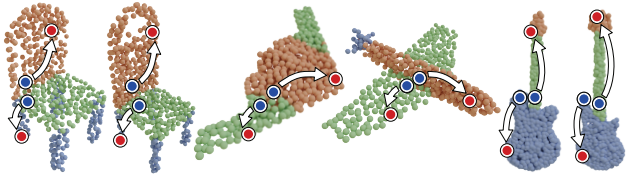
1. Introduction

Learning point features is one of the most fundamental problems in shape analysis and a key building block for classic vision tasks such as classification and segmentation. Conventional convolution employs fixed kernels of varying sizes to compute point features, while extensions to variable neighborhoods, which account for anisotropy [43] and other local shape properties, have also been studied. Another line of approaches follow the non-local means idea [5] by collecting features at points that are similar to each other.

Recently, the use of selective attention [38, 24, 39, 30, 29] has gained much success in computer vision. In a typical setting, an attentional network computes the feature of a point by pre-selecting [11, 42, 54] a set of nearest points



(a) Directional attention points (red) learned for shape classification task.



(b) Directional attention points (red) learned for shape segmentation task.

Figure 1: Directional attention points (red dots) learned for various original points (blue dots) for different tasks. For classification (a), the attention points exhibit within-class consistency, while facilitating discrimination between different classes: red dots on chair backs vs. those on tabletops. For segmentation (b), the learned attention points help discriminate close-by points that belong to different segments.

in the point’s neighborhood and learning the associated attention weights to capture additional contextual information through the weights to enrich the point feature. Another recent approach resorts to finding non-local neighbors [49] by considering points within a much larger neighborhood.

In this paper, we take the attention-based point feature learning to an extreme by introducing an attention mechanism that learns *one and only one* attention point for feature learning and enhancement to serve such tasks as classification and segmentation. Let us take the classification as an example and show how our attention module is incorporated into a classification network, such as Dynamic Graph CNN or DGCNN [42], that is based on point-wise convolutional feature processing and aggregation. We simply replace each original convolution layer in the network (i.e., EdgeConv in

the case of DGCNN) with a new convolution, which *combines* or *fuses* the feature at an input point with the feature at its associated attention point. We call the attention point a *directional* attention point, or DAP, for short, since it is obtained by adding to the original point a *learned offset vector*. These offset vectors are learned by minimizing the classification errors over the training point clouds.

The motivations behind our approach are two-fold. First, not all attentions are the same [3, 33], and second, not all tasks are the same. It is believed that human visual attention may be sequential [33], which would fit a recurrent attention model [29], and the attention map may be *prioritized* based on “goal- and stimulus-driven selection”, as well as “the lingering effects of past selection episodes” [3]. However, instead of keeping track of a set or a sequence of attention points, our work opts for the simplest choice: *one attention point* (per input point) only. Then, it is critical to find the “best” attention point, perhaps one with the highest priority, to maximize its impact. To this end, we *learn* where the attention point is, from training data, rather than pre-selecting it based on feature similarity as in the case of local means [5] and prior attentional networks [49, 54]. Also importantly, the learning is *task-dependent*.

As shown in Figure 1, the learned attention points appear to exhibit a certain level of semantic understanding, depending on the task at hand, owing to training by the respective semantic task. Indeed, if the right attention point is selected, perhaps “one point is all you need.” Further, we can observe that the attention points behave differently for different tasks, and they are not always points with similar features as the original points. A critical observation here is that for the purpose of feature enhancement, points with dissimilar features may be equally useful since they can provide *complementary* information.

We show that our attention mechanism can be easily incorporated into state-of-the-art point cloud classification and segmentation networks, such as PointNet++ [32], RSCNN [26], DGCNN [42], and KPConv [37]. We demonstrate through comprehensive tests that, on common benchmarks ModelNet40, ShapeNetPart, and S3DIS, our DAP-enabled networks, e.g., DAP-DGCNN, DAP-KPConv, etc., *consistently* produce improved accuracies over the respective original networks, as well as all other competitive alternative deep models, including attentional point cloud analysis networks, such as PointASNL [49] and PointWeb [54], which employ pre-selected sets of attention points. Particularly, DAP-DGCNN attains the highest classification accuracy of **93.9** on the ModelNet40 dataset. The consistent improvements are verified over varying point neighborhood sizes, train-test splits, and ways for feature integration.

2. Related Work

Deep learning on 3D point clouds. Inspired by the seminal work of PointNet [31], many deep neural networks have been developed to directly operate on points [34]. To overcome the inadequacy of PointNet on capturing local structures, PointNet++ [32] adopts a deep hierarchical feature learning mechanism that recursively employs PointNet to process point neighborhoods of increasing sizes. Later, PCNN [2] adapts image-based CNNs to the point cloud setting, leading to a permutation-invariant point feature learning. PointCNN [21] learns a transformation matrix to weight the input features associated with the input points and rearrange the points into a canonical permutation. A recent survey on this topic is available in [10].

Point feature learning. Point features play an important role to task performance. So, a majority of deep models on 3D point clouds focus on designing methods to extract better features, typically by exploiting a point’s local neighborhood. DGCNN [42] bases the neighboring relations of points on their distances in the feature space and aggregates pair-wise features to generate features for the center point. PointWeb [54] densely connects every pair of points in a local neighborhood, aiming at extracting point feature that better represents the local region around the center point.

Other methods focus on designing efficient convolution kernels [4, 17] on points. PointConv [44] treats the convolution kernel as a Monte Carlo estimate of nonlinear functions of the local 3D coordinates of points. Point features are weighted by the estimated density. KPConv [37] uses a set of points in Euclidean space as the convolution kernel and aggregates input features based on the distances between kernel points and input points. Liu et al. [27] reveal that different local operators contribute similarly to network performance. While prior works focus mostly on learning local features, some recent ones [8, 49] start to explore non-local 3D features with the attention mechanism [38].

Attentional point feature learning. Attention-based feature learning [38] has been introduced to learning point features soon after its applications to image features. Rather than being exhaustive, we discuss methods that focus on point feature learning rather than on specific vision tasks. Xie et al. [46] adopt self-attention to integrate point selection and feature aggregation into a single soft alignment operation. Yang et al. [50] propose the point attention transformer, which leverages a parameter-efficient group shuffle attention to learn the point relations. Zhang et al. [53] propose Point Contextual Attention Network to predict the significance of each local point feature based on the point context. Chen et al. [7] learn local geometric representations by embedding a graph attention mechanism.

Further, attention can be used to learn long-range global

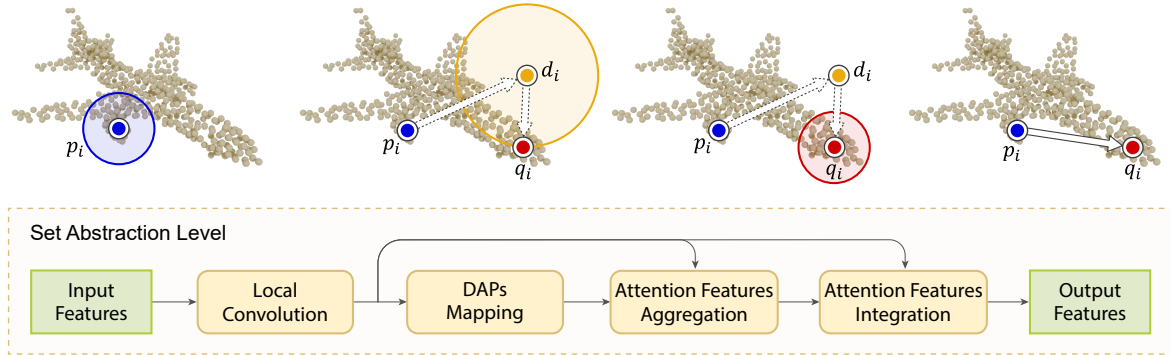


Figure 2: Learning directional attention point (DAP): an illustration. For a point p_i (blue point), its feature f_i is updated using arbitrary local convolution. After that, we take f_i to learn an offset vector to locate the offset point d_i (yellow point). With the point d_i , we further locate the target directional attention point q_i (red point). We then aggregate the neighboring features of point q_i and finally integrate the feature of the directional attention point into point p_i .

features. Liu et al. [23] propose Point2Sequence, an RNN-based model that captures correlations between different areas in a point cloud. Lu et al. [28] design the spatial-channel attention module to capture multi-scale and global context features. Han et al. [12] create a global graph and weights features of distant points with attention. More recently, Cheng et al. [8] propose global-level blocks to update the feature of a superpoint using weighted features of other superpoints, while Yan et al. [49] propose PointASNL that samples points over the whole point cloud to query similar ones for non-local point feature learning.

All the methods mentioned above *pre-select a set of points*, usually points in the local neighborhood or points with similar features, as the attentional points. In the 2D image domain, Zhang et al. [52] propose to learn an affinity matrix for each attention point to shift it to a better location. The features of the attention points are weighted based on feature similarity. On the other hand, Xue et al. [48] suggest that not all attention is needed, and only a small part of the inputs is related to the output targets, through their investigations into several natural language processing tasks. Our work is inspired by such learned attentions. Yet, we go beyond it and propose to *directly learn to find the point to attend to* without relying on the feature similarity. Importantly, we design a new network module to learn to generate an offset vector in the latent space and take it to locate the right attention point over the entire point cloud.

3. Method

Recent deep learning approaches for 3D point clouds often focus on designing operators for better local feature extraction. Denoting $f_i \in \mathbb{R}^{C_1}$ as the input feature of point p_i in a certain network layer (C_1 is the channel number), this local operator takes the input features of p_i 's neighbors and

aggregates them to form the output feature $f'_i \in \mathbb{R}^{C_2}$ of p_i

$$f'_i = \text{LocalConv}(\mathcal{N}(p_i)), \quad (1)$$

where $\mathcal{N}(p_i)$ is the set of neighboring points of p_i , which are often found by a ball query or k-nearest neighbor (KNN) search. Here, *LocalConv* denotes a local convolution. It can be a point-wise local operator [31, 32], a grid kernel local operator [37], or an attention-based local operator [54].

Some methods use attention to learn global features for long-range structures, in which $\mathcal{N}(p_i)$ is replaced by a set of pre-selected attention points. These points can be found by locating points with similar features as f_i in the feature space. Like Eq. (1), a basic mechanism is to weigh the input features of the attention points based on the feature similarity, then to combine them into the output feature of p_i .

In this work, we propose a new network module, called DAP-Conv, that *directly learns* to find attention points without relying on the feature similarity. In particular, we learn to find for each input point p_i *only one* attention point instead of finding multiple ones. The top part of Figure 2 illustrates how DAP-Conv works. Let P be the input cloud with n points $\{p_1, p_2, \dots, p_n\}$. Taking as an example the blue point in Figure 2 as p_i , we learn to find its associated directional attention point q_i , the red point, through the assistance of the offset point d_i , the yellow point. The bottom part of Figure 2 shows the overall feature learning pipeline. First, we update feature f_i of point p_i using a Local Convolution block (Eq. (1)), then map f_i to the corresponding directional attention point q_i using the DAPs Mapping block (Section 3.1). Next, the Attention Features Aggregation block (Section 3.2) aggregates features for the directional attention point q_i . Finally, the Attention Features Integration block (Section 3.3) integrates the feature of the directional attention point into the output feature of p_i . Also, we show the detailed structure of DAP-Conv in Figure 3, in

which the three blocks are outlined.

3.1. Learning Directional Attention Points

The features of points in the point cloud are first updated with Eq. (1). We learn a function D ('D' for directional) to map the input feature of point p_i to locate offset point d_i (the yellow point in Figure 2) with

$$d_i = D(f_i), \quad (2)$$

and then find the target directional attention point q_i (the red point) with the assistance of point d_i . Inspired by the way how neighboring points are found in the feature space [42], we propose to learn to find the directional attention points either in the Euclidean space or in the feature space.

Case (i). For directional attention points in the Euclidean space, we use a small MLP to map the feature f_i to a three-dimensional offset vector in the Euclidean space. We then add this vector back to the 3D coordinates x_i of the original point p_i to locate the offset point

$$d_i = MLP(f_i) + x_i. \quad (3)$$

This MLP is shared among all the points in the input point cloud P . Also, point d_i is not necessarily a point in P . Its location is arbitrary in the Euclidean space. Hence, we map the feature of point p_i to an offset vector, which acts as an attention direction for further pinpointing d_i . Taking point d_i as guidance, we then find the nearest point q_i to point d_i among all the points in the entire point cloud as the directional attention point q_i associated with p_i .

Case (ii). For directional attention points in the feature space, the feature f_i of point p_i is mapped via a small shared MLP to an offset vector (with same channel number as f_i) in the feature space. This vector is then added to f_i to produce f_{d_i} , which is an offset feature in the feature space:

$$f_{d_i} = MLP(f_i) + f_i. \quad (4)$$

Similar to d_i in case (i), offset feature f_{d_i} is not necessarily a feature vector of the points in the original point cloud. Also, it can have arbitrary values. With f_{d_i} , we then search the entire point cloud for point q_i with the nearest feature vector f_{q_i} to f_{d_i} in the feature space, and take q_i as the corresponding directional attention point of point p_i . The blocks with a red-dotted frame in Figure 3 illustrates the detailed procedure of this DAPs Mapping.

3.2. Attentional Features Aggregation

After finding the target directional attention point q_i for point p_i , we then aggregate the features of the neighborhood of q_i and update the feature of point q_i with

$$f_{q_i} = LocalConv(\mathcal{N}(q_i)). \quad (5)$$

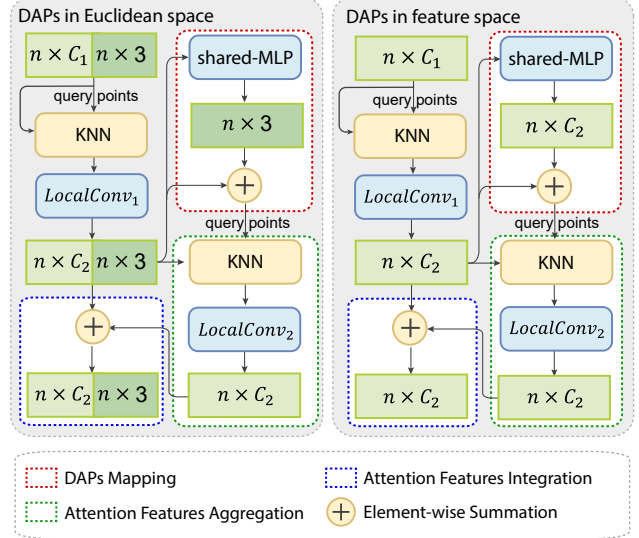


Figure 3: The structure of DAP-Conv. For directional attention points in the Euclidean space, we learn the 3-dimensions offset vectors and add them back. The resulting points are used as query points to find the k nearest points in the point cloud. The features of these points are aggregated into directional attention points and the features of these directional attention points are integrated into the original features. For directional attention points in the feature space, the offset vectors are in the same space and the neighboring points are also found in the feature space.

For directional attention points in the Euclidean space, these neighboring points are found in the Euclidean space. For directional attention points in the feature space, these neighboring points are also found in the feature space.

To find the closest point q_i to d_i , we need to calculate the distances between point d_i and all the other points. To further find the neighboring points of q_i , another distance calculation is required. To reduce the cost of processing two sets of distance calculations, we directly find the neighboring points of point d_i instead of explicitly finding point q_i and then its neighbors. The directional attention point q_i must be among the neighboring points of d_i , since q_i is the nearest one to d_i in the original point cloud. So, the feature of the directional attention point can be updated using the features of the neighboring points of d_i as

$$f_{q_i} = LocalConv(\mathcal{N}(d_i)). \quad (6)$$

For both cases (i) and (ii), we prefer to find these neighboring points using KNN. In this situation, no matter how large the offset vectors are, there are always neighboring points of d_i . If the neighboring points are found with a ball query [32], an additional loss is needed to punish the point d_i from being shifted too far away. Otherwise, there could

be no neighboring points of d_i within a certain radius.

Hence, we use KNN to finding the neighboring points for performing $LocalConv_1$ for consistency. After we learn the offset points, we use them as query points to find k neighboring points and update the feature of q_i , as shown in the green dotted frames in Figure 3. It should be noticed that all these neighboring points are points from the original point cloud (case (i)) or the features of the points in the original point cloud (case (ii)), in which d_i or f_{d_i} is not one of them.

3.3. Integration of Attentional Features

After we aggregate a feature for the directional attention point q_i , we then integrate the feature into the feature of p_i with an integration function I ('I' for integration):

$$f'_i = I(LocalConv_1(\mathcal{N}(p_i)), LocalConv_2(\mathcal{N}(d_i))), \quad (7)$$

where we could use the same or different convolutional operators for $LocalConv_1$ and $LocalConv_2$.

In the previous attention-based networks for processing point clouds, *e.g.*, [42, 54, 8, 49, 50, 12, 46, 22], the features of the attention points are weighted by a dot-product similarity between the features of the pre-selected attention points and p_i , or by the similarity in the spatial location between them. An attention point with a more similar feature is given a larger weight when added into the feature of p_i . However, we argue that *not only* points with similar features could be useful, *but also* points with *different features* could also be useful in feature learning. Particularly, points with different features could supply the center point p_i with *vital context for performing the target task*.

Here, one straightforward choice for I is to simply add the features of point q_i and point p_i together:

$$I = Add(f_{p_i}, f_{q_i}), \quad (8)$$

as illustrated in the blue dotted frames in Figure 3. Since $LocalConv_1$ and $LocalConv_2$ do not share parameters, the network can learn to update the feature of q_i for adding it into the feature of p_i . Another choice for I is to concatenate the two features then use an MLP to reduce the dimensions:

$$I = MLP(Concatenate(f_{p_i}, f_{q_i})). \quad (9)$$

A comparison result between these two forms of feature integration can be found in Table 5 of Section 4.

4. Results and Evaluation

Our proposed DAP-Conv can be easily adapted into conventional point-wise feature learning networks. In existing networks, a $LocalConv$ block is generally used in a set abstraction level to update the input feature f_i of a point and produce f'_i , as described in Eq. (1). Hence, by keeping the channel sizes of the input and output features to be the same,

Table 1: 3D Shape classification results on ModelNet40. OA: overall accuracy (%); mAcc: mean class accuracy (%); xyz: points only as input; xyz+nor: use points and normals.

Method	input	#points	OA
O-CNN [40]	xyz+nor	-	90.6
Kd-Net [16]	xyz	32k	91.8
SpiderCNN [47]	xyz+nor	5k	92.4
KPConv [37]	xyz	7k	92.9
SO-Net [19]	xyz+nor	5k	93.4
PointNet [32]	xyz	1k	89.2
PAT [50]	xyz+nor	1k	91.7
PointCNN [21]	xyz	1k	92.2
PCNN [2]	xyz	1k	92.3
PointWeb [54]	xyz+nor	1k	92.3
PointConv [44]	xyz+nor	1k	92.5
A-CNN [17]	xyz	1k	92.6
Point2Node [12]	xyz	1k	93.0
PointASNL [49]	xyz	1k	92.9
PointASNL [49]	xyz+nor	1k	93.2
DensePoint [25]	xyz	1k	93.2
PointNet++ [32]	xyz	1k	90.7
RSCNN [26]	xyz	1k	91.7
DGCNN [42]	xyz	1k	92.9
DAP-PointNet++	xyz	1k	92.9
DAP-RSCNN	xyz	1k	92.8
DAP-DGCNN	xyz	1k	93.9

we can replace the $LocalConv$ block in existing networks with our DAP-Conv to boost the network performance.

To demonstrate the effectiveness of our DAP-Conv, we adapt it into common networks, including PointNet++ [32], RSCNN [26], DGCNN [42], and KPConv [37], producing DAP-enabled networks, *i.e.*, DAP-PointNet++, DAP-RSCNN, DAP-DGCNN, and DAP-KPConv. We conduct experiments using these networks on various tasks, including shape classification (Section 4.1), part segmentation, and semantic segmentation (Section 4.2), showing both quantitative comparisons and qualitative results. At last, we evaluate various aspects of our DAP-Conv (Section 4.3), *e.g.*, one vs. multiple directional attention points, neighborhood sizes, train/test split, etc.

4.1. Classification

First, we evaluate our method on the shape classification task using ModelNet40 [45], which provides a comprehensive collection of 12,311 CAD models from 40 categories. Here, we use the input point clouds sampled from these models by PointNet [31]. Typically, 1,024 points are uniformly sampled per model to serve as the network input. Following the official train/test split, we use 9,843 models for training and 2,468 models for testing.

Table 2: Part segmentation results on ShapeNet Part.

Method	mIoU
Kd-Net [16]	82.3
PointNet [31]	83.7
PointNet++ [32]	85.1
PCNN [2]	85.1
DGCNN [42]	85.2
DAP-PointNet++	85.2
DAP-DGCNN	85.8

In this experiment, we evaluate the performance of DAP-PointNet++, DAP-RSCNN, and DAP-DGCNN, where data preprocessing, augmentation, and hyper-parameters all follow the original network settings. Also, we employ only 3D point coordinates as network inputs.

For DAP-PointNet++, we use DAP-Conv in the first set abstraction level with another shared-MLP to further fuse features, where feature integration is carried out as in Eq. (9). Note that *LocalConv*₁ and *LocalConv*₂ in Figure 3 are small shared-MLPs with max-pooling separately.

For DAP-RSCNN, we also use DAP-Conv in the first set abstraction level; *LocalConv*₁ is an RS-Conv and *LocalConv*₂ is a small shared-MLP with max-pooling. Note that, since only the single-scale version of the RSCNN code is officially released, we develop our DAP-RSCNN based on the released code and report 91.7 for the single-scale RSCNN, following [20].

Finally, for DAP-DGCNN, we replace all the four EdgeConv blocks with DAP-Conv and use EdgeConv for *LocalConv*₁ and *LocalConv*₂.

Table 1 reports the results of using different methods for the shape classification task. Comparing the results of the three DAP-enabled networks with those of the original counterparts, we can see that all of them improve the performance over the original networks, showing that our DAP-Conv can help improve the quality of the features for the shape classification task. Excitingly, DAP-DGCNN attains the highest performance with an overall accuracy of 93.9 on the classification task, compared with all others, including some very recent methods such as PointASNL [49].

4.2. Segmentation

Part segmentation. The ShapeNet Part dataset [51] has 16,881 shapes over 16 categories and with 50 part labels. We sample 2,048 points per shape from this dataset for our experiments and follow the official data split setup [6] adopted in DGCNN [42] and PointNet++ [32].

All the DAP-Conv blocks employed for part segmentation and semantic segmentation are followed with a small MLP to further fuse features from different semantic parts. For DAP-PointNet++, we use the same adaptation as for

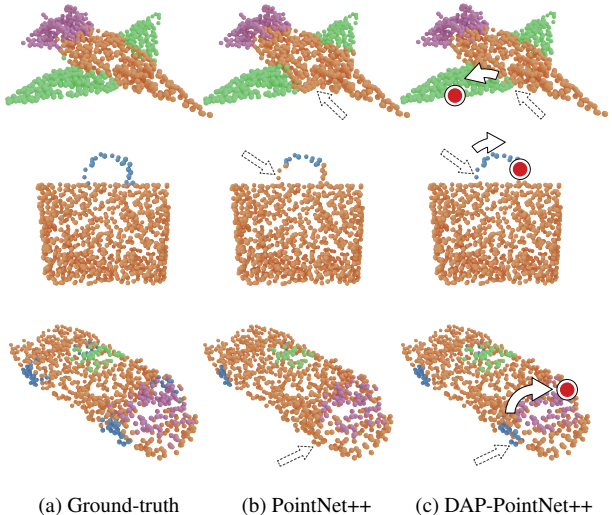


Figure 4: Comparing part segmentation on ShapeNet Part between PointNet++ and DAP-PointNet++. In each case, we highlight an incorrectly labeled point near a segmentation boundary (*hollow arrow*) by PointNet++ and how the use of DAP-Conv (right) corrected the label with feature enhancement by an attention point (large red dot).

shape classification. For DAP-DGCNN, we replace the second and third set abstraction levels with our DAP-Conv. Table 2 reports the performance achieved by various methods (in terms of the mean Intersection-over-Union (mIoU) metric), showing that DAP-Conv helps improve the part segmentation performance of PointNet++ and DGCNN. Figure 4 visually contrasts PointNet++ and DAP-PointNet++ to show the differences made by DAP-Conv. More such results can be found in the supplementary material.

Indoor scene semantic segmentation. We use the Stanford 3D Large-Scale Indoor Spaces (S3DIS) dataset [1], which contains large-scale 3D-scanned point clouds for six indoor areas with 272 rooms from three different buildings. Altogether, the dataset has around 273 million points, each belonging to one of 13 semantic categories. Area-5 is used as the test scene for evaluating the method generalizability.

For DAP-DGCNN, each room is split into blocks of size $1m \times 1m$. The input is point coordinates together with RGB colors and normalized spatial coordinates (a 9D vector per point), following the settings in DGCNN [42]. During the training, we sample 4,096 points from each room block. Then, all sampled points are used for testing. The second set abstraction level of DGCNN is replaced by DAP-Conv for semantic segmentation. For DAP-KPConv, the last two KPConv blocks are replaced by DAP-Conv. Each 3D scene in the dataset is segmented into small sub-clouds contained

Table 3: Semantic segmentation results on the S3DIS dataset (evaluated on Area 5).

Method	mIoU
PointNet [31]	41.1
DGCNN [42]	49.1
TangentConv [36]	52.6
PointCNN [21]	57.3
SPGraph [18]	58.0
ParamConv [41]	58.3
PointWeb [54]	60.3
HPEIN [15]	61.9
MVPNet [14]	62.4
Point2Node [12]	63.0
MinkowskiNet [9]	65.4
KPConv rigid [37]	65.4
KPConv deform [37]	67.1
JSENNet [13]	67.7
DAP-DGCNN	53.6
DAP-KPConv rigid	67.3
DAP-KPConv deform	68.2

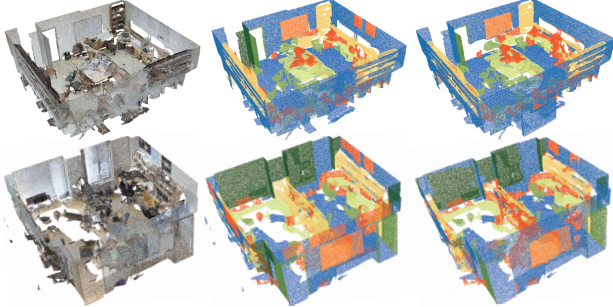


Figure 5: Visualization of two semantic segmentation results on S3DIS. Left: input point cloud with RGB colors. Middle: points with ground-truth semantic labels. Right: segmentation results predicted by DAP-DGCNN.

in spheres. During the training, the spheres are picked randomly in the scenes, and during the testing, the spheres are picked regularly in the point clouds. Table 3 gives the results, showing that DAP-Conv helps improve the semantic segmentation performance on S3DIS for both DGCNN and KPConv. Also, we present two of the visual semantic segmentation results on S3DIS in Figure 5.

4.3. Ablation Study

Finally, we evaluate various aspects of our method, employing DAP-DGCNN to test on ModelNet40.

Different options for choosing DAPs. In this experiment, we compare DAP-DGCNN with three variants of choosing attention points: (i) random-DAP-DGCNN, in which we replace the MLP for learning to generate the off-

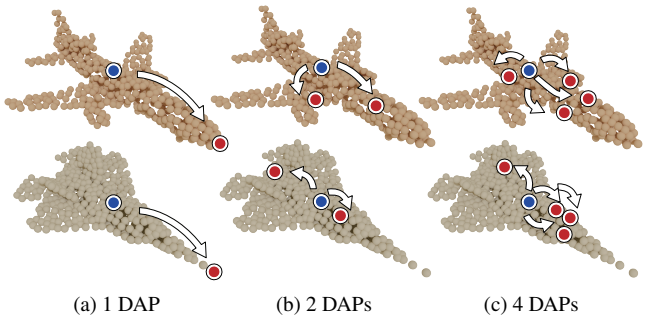


Figure 6: Visualization of the DAPs (red dots) selected by networks which learn different number of attention points. The two airplane shapes, top and bottom rows, are different but structurally similar. The DAPs were selected for the *same* original point (blue dot) in each row.

Table 4: Comparing different ways of choosing DAPs.

	OA	mAcc
DGCNN (baseline)	92.9	90.2
random-DAP-DGCNN	93.0	89.9
DAP2-DGCNN	93.3	90.2
DAP4-DGCNN	93.1	90.3
DAP-DGCNN	93.9	91.5

sets (Eq. (3) & Eq. (4)) with a randomly-generated vector, thus replacing the core of our DAP-Conv (which uses the learned offset vector to locate the directional attention point); and (ii) DAP2-DGCNN and DAP4-DGCNN, which learns two and four directional attention points (instead of one), respectively.

As comparison results in Table 4 show, random-DAP-DGCNN hardly makes any improvement over the baseline, which is DGCNN. This result demonstrates the importance of the learned offset vectors for searching for the directional attention point. Yet, using just the right directional attention point, as in DAP-DGCNN, we can achieve a large performance improvement over the original DGCNN.

Next, comparing DAP2-DGCNN and DAP4-DGCNN with DAP-DGCNN, we can see that learning to find and use more than one directional attention points improves over DGCNN. However, the improvement is far below than using just one single directional attention point. Yet, an interesting observation is that the more directional attention points we use, the worse the result is. The visualization in Figure 6 on where the 1, 2, and 4 attention points were selected by the networks may hint at a possible reason: as more points are added, their consistency tends to drop.

Different feature integration. We can have different ways of integrating the feature of point p_i with that of its

Table 5: Comparing different ways of integrating features.

Different Function I	OA	mAcc
I_1 or Eq. (8)	93.9	91.5
I_2 or Eq. (9)	93.6	91.0

Table 6: Comparing different neighboring sizes (k) in KNN.

k	OA	
	DGCNN	DAP-DGCNN
5	90.5	93.5
10	91.4	93.4
20	92.9	93.9
40	92.4	93.3

Table 7: Shape classification results on ModelNet40 with different train/test splits.

(Train/all)%	OA	
	DGCNN	DAP-DGCNN
80%	92.9	93.9
60%	91.5	92.6
40%	90.6	92.1
20%	88.9	90.2
10%	87.3	88.0
5%	82.7	83.1
1%	63.5	64.9

DAP q_i ; see Section 3.3. As shown in Table 5, option I_1 (Eq. (8)) gives a slightly better performance compared with I_2 (Eq. (9)), so we empirically choose I_1 in our DAP-Conv. We have tested other ways of feature integration, *e.g.*, point-wise multiply, but they do not lead to good results.

Different neighborhood sizes. Note that we built DAP-DGCNN by following the setting of DGCNN to use $k=20$ for the two KNN operations in DAP-Conv. In this experiment, we test DAP-DGCNN with different neighborhood sizes (k), while keeping all the other settings unchanged.

As shown by results in Table 6, the performance of our DAP-DGCNN is quite robust against different choices of k , and it also consistently outperforms DGCNN. Even with a rather small neighborhood size $k=5$, our method can already attain a rather high performance, which exceeds that of DGCNN for all the neighborhood sizes shown in Table 6, *as well as* all other methods listed in Table 1.

Different train/test splits. In a final experiment, we test the robustness of our method over different training/test splits. Note that the original setting uses 9,843 models, which is around 80% of the whole dataset, for training, and the remaining 20% for testing. We test the performance of our DAP-DGCNN using smaller training sets, from 80% down to 1% of the whole dataset, and compare to DGCNN,

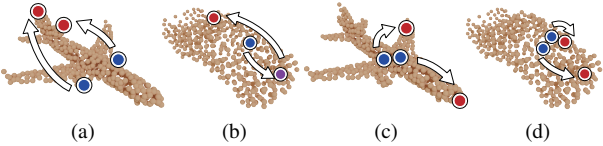


Figure 7: DAP selection learned by our network is neither symmetric (a) nor invertible (b), in general; and it is not always stable (c-d), as nearby points may be mapped afar.

with results shown in Table 7. Similar to [35], we select the training samples as follows, for all train/test splits: we randomly sample one object per class first; the remaining training data are randomly sampled from the original training set, regardless of their classes. As we can observe from Table 7, our method performs well even with a very small training set, and most importantly, it consistently outperforms DGCNN over all train/test splits. Also, the randomization during our setup of the multiple training sets can alleviate potential concerns of over-fitting.

5. Discussion, Limitation, and Future Work

“One Attention Point is All You Need.” This is the key message from our work, in the context of selecting attention points to enhance point features for classical shape analysis tasks such as point cloud classification and segmentation. As the results in Table 4 show, more DAPs, which were learned in the same manner as in our single-DAP network, appear to degrade performance. We speculate that as geometries and structures vary, *e.g.*, within the same class of shapes for classification or within the same semantic part in the context of segmentation, it is the easiest to attain *consistency* with the first DAP. This is less so when two DAPs are identified, and even harder with four DAPs; see Figure 6 for partial evidence. Therefore, more DAPs may “contaminate” the results. We would like to investigate and validate this phenomenon more formally in future work.

Currently, the learned DAP selection is *neither symmetric nor invertible* in general. As shown in Figure 7, if two points p and q are symmetric on a shape, $DAP(p)$ and $DAP(q)$ may not be; and $p \neq DAP(DAP(p))$. The figure also shows that the selection may become unstable, as one would expect from the results of a data-driven optimization. However, it is worth noting that in general, we find the learned offset vectors to be more stable than the final attention points, which are obtained by projecting back onto the point clouds. These findings suggest that we do not yet have a mathematically or semantically precise way to reason about the best attention point. As our current learning framework is completely data-driven, adding an inductive bias to enforce consistency would be worth exploring.

On the technical front, our method may not extend to

other representations such as voxels. In voxel-based representation, the offset points need to be discretized into voxels which may cause discontinuity in gradients. Another limitation is the inherent computational cost in computing dynamic offset vectors. Since the learned offset points are not in the original point cloud, we have to compute point distances on the fly. Consequently, it is impossible to pre-compute the distances involving offset points for accelerating the training. Future remedies are worth considering.

References

- [1] Iro Armeni, Ozan Sener, Amir R. Zamir, Helen Jiang, Ioannis Brilakis, Martin Fischer, and Silvio Savarese. 3D semantic parsing of large-scale indoor spaces. In *Proc. IEEE Conf. on Computer Vision & Pattern Recognition*, pages 1534–1543, 2016. [6](#)
- [2] Matan Atzmon, Haggai Maron, and Yaron Lipman. Point convolutional neural networks by extension operators. *ACM Trans. on Graphics (Proc. SIGGRAPH)*, 37(4):1–12, 2018. [2, 5, 6](#)
- [3] Edward Awh, Artem V. Belopolsky, and Jan Theeuwes. Top-down versus bottom-up attentional control: a failed theoretical dichotomy. *Trends in Cognitive Sciences*, 16(8):437–443, 2012. [2](#)
- [4] Alexandre Boulch. ConvPoint: Continuous convolutions for point cloud processing. *Computers & Graphics*, 88:24–34, 2020. [2](#)
- [5] Antoni Buades, Bartomeu Coll, and J.-M. Morel. A non-local algorithm for image denoising. In *Proc. IEEE Conf. on Computer Vision & Pattern Recognition*, volume 2, pages 60–65. IEEE, 2005. [1, 2](#)
- [6] Angel X. Chang, Thomas Funkhouser, Leonidas Guibas, Pat Hanrahan, Qixing Huang, Zimo Li, Silvio Savarese, Manolis Savva, Shuran Song, Hao Su, et al. ShapeNet: An information-rich 3D model repository. *arXiv preprint arXiv:1512.03012*, 2015. [6](#)
- [7] Can Chen, Luca Zanotti Fragonara, and Antonios Tsourdos. GAPNet: Graph attention based point neural network for exploiting local feature of point cloud. *arXiv preprint arXiv:1905.08705*, 2019. [2](#)
- [8] Mingmei Cheng, Le Hui, Jin Xie, Jian Yang, and Hui Kong. Cascaded non-local neural network for point cloud semantic segmentation. *arXiv preprint arXiv:2007.15488*, 2020. [2, 3, 5](#)
- [9] Christopher Choy, JunYoung Gwak, and Silvio Savarese. 4D spatio-temporal ConvNets: Minkowski convolutional neural networks. In *Proc. IEEE Conf. on Computer Vision & Pattern Recognition*, pages 3075–3084, 2019. [7](#)
- [10] Yulan Guo, Hanyun Wang, Qingyong Hu, Hao Liu, Li Liu, and Mohammed Bennamoun. Deep learning for 3D point clouds: A survey. *IEEE Trans. Pattern Analysis & Machine Intelligence*, 2020. [2](#)
- [11] Will Hamilton, Zhitao Ying, and Jure Leskovec. Inductive representation learning on large graphs. In *Proc. Conf. on Neural Information Processing Systems*, pages 1024–1034, 2017. [1](#)
- [12] Wenkai Han, Chenglu Wen, Cheng Wang, Xin Li, and Qing Li. Point2Node: Correlation learning of dynamic-node for point cloud feature modeling. In *Proc. AAAI Conf. on Artificial Intelligence*, pages 10925–10932, 2020. [3, 5, 7](#)
- [13] Zeyu Hu, Mingmin Zhen, Xuyang Bai, Hongbo Fu, and Chiew-lan Tai. JSENet: Joint semantic segmentation and edge detection network for 3D point clouds. *Proc. Euro. Conf. on Computer Vision*, 2020. [7](#)
- [14] Maximilian Jaritz, Jiayuan Gu, and Hao Su. Multi-view pointnet for 3D scene understanding. In *Proc. of the IEEE Int. Conf. on Computer Vision Workshops*, pages 0–0, 2019. [7](#)
- [15] Li Jiang, Hengshuang Zhao, Shu Liu, Xiaoyong Shen, Chi-Wing Fu, and Jiaya Jia. Hierarchical point-edge interaction network for point cloud semantic segmentation. In *Proc. IEEE Conf. on Computer Vision & Pattern Recognition*, pages 10433–10441, 2019. [7](#)
- [16] Roman Klokov and Victor Lempitsky. Escape from cells: Deep Kd-networks for the recognition of 3D point cloud models. In *Proc. Int. Conf. on Computer Vision*, pages 863–872, 2017. [5, 6](#)
- [17] Artem Komarichev, Zichun Zhong, and Jing Hua. A-CNN: Annularly convolutional neural networks on point clouds. In *Proc. IEEE Conf. on Computer Vision & Pattern Recognition*, pages 7421–7430, 2019. [2, 5](#)
- [18] Loic Landrieu and Martin Simonovsky. Large-scale point cloud semantic segmentation with superpoint graphs. In *Proc. IEEE Conf. on Computer Vision & Pattern Recognition*, pages 4558–4567, 2018. [7](#)
- [19] Jiaxin Li, Ben M. Chen, and Gim Hee Lee. SO-Net: Self-organizing network for point cloud analysis. In *Proc. IEEE Conf. on Computer Vision & Pattern Recognition*, pages 9397–9406, 2018. [5](#)
- [20] Ruihui Li, Xianzhi Li, Pheng-Ann Heng, and Chi-Wing Fu. PointAugment: an auto-augmentation framework for point cloud classification. In *Proc. IEEE Conf. on Computer Vision & Pattern Recognition*, pages 6378–6387, 2020. [6](#)
- [21] Yangyan Li, Rui Bu, Mingchao Sun, Wei Wu, Xinhua Di, and Baoquan Chen. PointCNN: Convolution on χ -transformed points. In *Proc. Conf. on Neural Information Processing Systems*, pages 820–830, 2018. [2, 5, 7](#)
- [22] Zhidong Liang, Ming Yang, and Chunxiang Wang. 3D graph embedding learning with a structure-aware loss function for point cloud semantic instance segmentation. *arXiv preprint arXiv:1902.05247*, 2019. [5](#)
- [23] Xinhai Liu, Zhizhong Han, Yu-Shen Liu, and Matthias Zwicker. Point2Sequence: Learning the shape representation of 3D point clouds with an attention-based sequence to sequence network. In *Proc. AAAI Conf. on Artificial Intelligence*, volume 33, pages 8778–8785, 2019. [3](#)
- [24] Xiao Liu, Tian Xia, Jiang Wang, Yi Yang, Feng Zhou, and Yuanqing Lin. Fully convolutional attention networks for fine-grained recognition. *arXiv preprint arXiv:1603.06765*, 2016. [1](#)
- [25] Yongcheng Liu, Bin Fan, Gaofeng Meng, Jiwen Lu, Shiming Xiang, and Chunhong Pan. DensePoint: Learning densely contextual representation for efficient point cloud process-

ing. In *Proc. Int. Conf. on Computer Vision*, pages 5239–5248, 2019. 5

[26] Yongcheng Liu, Bin Fan, Shiming Xiang, and Chunhong Pan. Relation-shape convolutional neural network for point cloud analysis. In *Proc. IEEE Conf. on Computer Vision & Pattern Recognition*, pages 8895–8904, 2019. 2, 5

[27] Ze Liu, Han Hu, Yue Cao, Zheng Zhang, and Xin Tong. A closer look at local aggregation operators in point cloud analysis. *Proc. Euro. Conf. on Computer Vision*, 2020. 2

[28] Haihua Lu, Xuesong Chen, Guiying Zhang, Qiuha Zhou, Yanbo Ma, and Yong Zhao. SCANet: Spatial-channel attention network for 3D object detection. In *Proc. Int. Conf. on Acoustics, Speech & Signal Processing*, pages 1992–1996. IEEE, 2019. 3

[29] Volodymyr Mnih, Nicolas Heess, Alex Graves, et al. Recurrent models of visual attention. In *Proc. Conf. on Neural Information Processing Systems*, pages 2204–2212, 2014. 1, 2

[30] Y. Peng, X. He, and J. Zhao. Object-part attention model for fine-grained image classification. *IEEE Trans. on Image Processing*, 27(3):1487–1500, 2018. 1

[31] Charles R. Qi, Hao Su, Kaichun Mo, and Leonidas J. Guibas. PointNet: Deep learning on point sets for 3D classification and segmentation. In *Proc. IEEE Conf. on Computer Vision & Pattern Recognition*, pages 652–660, 2017. 2, 3, 5, 6, 7

[32] Charles R. Qi, Li Yi, Hao Su, and Leonidas J. Guibas. PointNet++: Deep hierarchical feature learning on point sets in a metric space. In *Proc. Conf. on Neural Information Processing Systems*, pages 5099–5108, 2017. 2, 3, 4, 5, 6

[33] Ronald A. Rensink. The dynamic representation of scenes. *Visual Cognition*, 7:17–42, 2000. 2

[34] Gernot Riegler, Ali Osman Ulusoy, and Andreas Geiger. OctNet: Learning deep 3D representations at high resolutions. In *Proc. IEEE Conf. on Computer Vision & Pattern Recognition*, pages 3577–3586, 2017. 2

[35] Jonathan Sauder and Bjarne Sievers. Self-supervised deep learning on point clouds by reconstructing space. In *Proc. Conf. on Neural Information Processing Systems*, pages 12962–12972, 2019. 8

[36] Maxim Tatarchenko, Jaesik Park, Vladlen Koltun, and Qian-Yi Zhou. Tangent convolutions for dense prediction in 3D. In *Proc. IEEE Conf. on Computer Vision & Pattern Recognition*, pages 3887–3896, 2018. 7

[37] Hugues Thomas, Charles R. Qi, Jean-Emmanuel Deschaud, Beatriz Marcotegui, François Goulette, and Leonidas J. Guibas. KPConv: Flexible and deformable convolution for point clouds. In *Proc. Int. Conf. on Computer Vision*, pages 6411–6420, 2019. 2, 3, 5, 7

[38] Ashish Vaswani, Noam Shazeer, Niki Parmar, Jakob Uszkoreit, Llion Jones, Aidan N. Gomez, Łukasz Kaiser, and Illia Polosukhin. Attention is all you need. In *Proc. Conf. on Neural Information Processing Systems*, pages 5998–6008, 2017. 1, 2

[39] Fei Wang, Mengqing Jiang, Chen Qian, Shuo Yang, Cheng Li, Honggang Zhang, Xiaogang Wang, and Xiaou Tang. Residual attention network for image classification. In *Proc. IEEE Conf. on Computer Vision & Pattern Recognition*, pages 3156–3164, 2017. 1

[40] Peng-Shuai Wang, Yang Liu, Yu-Xiao Guo, Chun-Yu Sun, and Xin Tong. O-CNN: Octree-based convolutional neural networks for 3D shape analysis. *ACM Trans. on Graphics (Proc. SIGGRAPH)*, 36(4):1–11, 2017. 5

[41] Shenlong Wang, Simon Suo, Wei-Chiu Ma, Andrei Pokrovsky, and Raquel Urtasun. Deep parametric continuous convolutional neural networks. In *Proc. IEEE Conf. on Computer Vision & Pattern Recognition*, pages 2589–2597, 2018. 7

[42] Yue Wang, Yongbin Sun, Ziwei Liu, Sanjay E. Sarma, Michael M. Bronstein, and Justin M. Solomon. Dynamic graph CNN for learning on point clouds. *ACM Trans. on Graphics*, 38(5):146, 2019. 1, 2, 4, 5, 6, 7

[43] Joachim Weickert. *Anisotropic diffusion in image processing*. B. G. Teubner (Stuttgart), 1998. 1

[44] Wenxuan Wu, Zhongang Qi, and Li Fuxin. PointConv: Deep convolutional networks on 3D point clouds. In *Proc. IEEE Conf. on Computer Vision & Pattern Recognition*, pages 9621–9630, 2019. 2, 5

[45] Zhirong Wu, Shuran Song, Aditya Khosla, Fisher Yu, Lin-guang Zhang, Xiaoou Tang, and Jianxiong Xiao. 3D ShapeNets: A deep representation for volumetric shapes. In *Proc. IEEE Conf. on Computer Vision & Pattern Recognition*, pages 1912–1920, 2015. 5

[46] Saining Xie, Sainan Liu, Zeyu Chen, and Zhuowen Tu. Attentional ShapeContextNet for point cloud recognition. In *Proc. IEEE Conf. on Computer Vision & Pattern Recognition*, pages 4606–4615, 2018. 2, 5

[47] Yifan Xu, Tianqi Fan, Mingye Xu, Long Zeng, and Yu Qiao. SpiderCNN: Deep learning on point sets with parameterized convolutional filters. In *Proc. Euro. Conf. on Computer Vision*, pages 87–102, 2018. 5

[48] Lanqing Xue, Xiaopeng Li, and Nevin L. Zhang. Not all attention is needed: Gated attention network for sequence data. In *Proc. AAAI Conf. on Artificial Intelligence*, pages 6550–6557, 2020. 3

[49] Xu Yan, Chaoda Zheng, Zhen Li, Sheng Wang, and Shuguang Cui. PointASNL: Robust point clouds processing using nonlocal neural networks with adaptive sampling. In *Proc. IEEE Conf. on Computer Vision & Pattern Recognition*, pages 5589–5598, 2020. 1, 2, 3, 5, 6

[50] Jiancheng Yang, Qiang Zhang, Bingbing Ni, Linguo Li, Jinxian Liu, Mengdie Zhou, and Qi Tian. Modeling point clouds with self-attention and Gumbel subset sampling. In *Proc. IEEE Conf. on Computer Vision & Pattern Recognition*, pages 3323–3332, 2019. 2, 5

[51] Li Yi, Vladimir G. Kim, Duygu Ceylan, I-Chao Shen, Mengyan Yan, Hao Su, Cewu Lu, Qixing Huang, Alla Sheffer, and Leonidas Guibas. A scalable active framework for region annotation in 3D shape collections. *ACM Trans. on Graphics (Proc. SIGGRAPH Asia)*, 35(6):1–12, 2016. 6

[52] Li Zhang, Dan Xu, Anurag Arnab, and Philip H.S. Torr. Dynamic graph message passing networks. In *Proc. IEEE Conf. on Computer Vision & Pattern Recognition*, pages 3726–3735, 2020. 3

[53] Wenxiao Zhang and Chunxia Xiao. PCAN: 3D attention map learning using contextual information for point cloud based

retrieval. In *Proc. IEEE Conf. on Computer Vision & Pattern Recognition*, pages 12436–12445, 2019. [2](#)

[54] Hengshuang Zhao, Li Jiang, Chi-Wing Fu, and Jiaya Jia. PointWeb: Enhancing local neighborhood features for point cloud processing. In *Proc. IEEE Conf. on Computer Vision & Pattern Recognition*, pages 5565–5573, 2019. [1](#), [2](#), [3](#), [5](#), [7](#)